ISSN 0023-1584, Kinetics and Catalysis, 2010, Vol. 51, No. 2, pp. 318–324. © Pleiades Publishing, Ltd., 2010.
Original Russian Text © A.V. Toktarev, L.V. Malysheva, E.A. Paukshtis, 2010, published in Kinetika i Kataliz, 2010, Vol. 51, No. 2, pp. 336–343.

Effect of Thermal Treatment Conditions on the Acid Properties of Zeolite Beta

A. V. Toktarev, L. V. Malysheva, and E. A. Paukshtis
Boreskov Institute of Catalysis, Siberian Branch, Russian Academy of Sciences, Novosibirsk, 630090 Russia
e-mail: malysh@catalysis.nsk.su

Received December 18, 2008

Abstract—The acid properties of zeolite Beta were studied by IR spectroscopy with the use of adsorbed NH_3 and CO probe molecules. It was found that the strength of the Brønsted acid sites (BASs) of zeolite Beta was the same as that of zeolite ZSM-5. Approximately a third of the total amount of BASs participated in the formation of hydrogen bonds at interdomain boundaries; thus, they were inaccessible to molecules larger than the ammonia molecule. The qualitative and quantitative compositions of acid sites in zeolite Beta can be regulated by changing the conditions of calcination of the initial zeolite form (temperature and/or gas atmosphere). Calcination under vacuum conditions afforded the highest acidity of the zeolite with respect to all types of acid sites. Calcination in a flow of air resulted in the lowest acidity of the sample, especially, with respect to the concentration of strong Lewis acid sites, because of the formation of an alumina phase. Calcination in an atmosphere of helium resulted in a decrease (as compared with a vacuum) in the rate of removal of the organic template decomposition products of the initial zeolite form from the channel volume. The resulting ethylene was mainly adsorbed at strong Lewis sites and converted into undesorbed condensation products.

DOI: 10.1134/S0023158410020229

INTRODUCTION

Zeolite Beta [1] is of considerable interest to both scientific research and industry. Zeolite Beta was first synthesized in 1967 [2], and its structure was determined only in 1988 [3]. Having a three-dimensional system of channels formed by twelve-membered rings of size 5.7 × 7.7 Å [4] and a framework composition varied over a wide range [2, 5], zeolite Beta combines the main advantages of commercially important zeolites such as Y and ZSM-5. Thus, it is believed that zeolite Beta can be used for the catalytic conversion of large molecules. Of course, the architecture and composition of a zeolite framework are responsible for the high activity and selectivity and the long lifetime of a zeolite catalyst chosen for a particular reaction. The nature, strength, concentration, and localization of acid sites are also of paramount importance. Usually, attention has been focused on the effect of the chemical composition of the framework of zeolite Beta on catalytic properties [1, 6].

The acidity of zeolite Beta, as well as other zeolites, was the subject matter of many studies [7, 8]. Acidic bridging (3608 cm^{-1}) and silanol (3740 cm^{-1}) OH^- groups [7] and Al–OH groups (3780 and 3680 cm^{-1}) [9, 10] occur on the surface of zeolite Beta, and the ratio between the intensities of IR bands due to these groups depends on the zeolite composition, preparation procedure, and subsequent thermal treatment conditions [11, 12].

The acidity of zeolites was measured by IR spectroscopy using the adsorption of probe molecules, which were strong (ammonia and pyridine) and weak bases (carbon monoxide, ethylene, and benzene). Because the frequency ν(CO) was found the most sensitive to the strength of acid sites, the IR spectra of adsorbed CO were commonly used for studying acid sites [13–16]. From a comparison between shifts in the bands of OH groups interacting with adsorbed molecules, it was found that the bridging OH groups of zeolites Beta and HZSM-5 were similar in strength, and the concentration of sites was proportional to the aluminum content of zeolite [17–19].

It was found using ^{27}Al NMR spectroscopy that almost all of the aluminum atoms in zeolite NH_4-Beta occurred in the tetrahedral positions of the zeolite lattice. Upon the calcination of NH_4-Beta, aluminum atoms can escape from the lattice to different extents because of zeolite lattice degradation; in this case, the coordination of aluminum escaped from the framework was octahedral [20].

Note that many studies of the acid properties of zeolites, in particular, zeolite Beta, made it possible to perform only a qualitative comparison between acid properties in individual series. The reason is the absence of integral absorption coefficients for the bands of adsorbed probe molecules, which allow one to determine the concentrations of acid sites of different strengths.

The preparation of a zeolite catalyst consists of a number of consecutive steps, each of them affects the nature and/or concentration of active sites. As a rule, the first step in the preparation of a high-silica zeolite catalyst is the thermal treatment of zeolite powder obtained after synthesis in order to anneal the organic constituent of the initial zeolite form. In this work, we attempted to determine a relationship between the conditions of the thermal treatment of the initial form of zeolite Beta and the nature and distribution of the resulting acid sites in the zeolite by IR spectroscopy with the use of probe molecules.

EXPERIMENTAL

Preparation of Zeolite Beta

The following reagents were used to prepare zeolite Beta: sodium aluminate (49.0% Al_2O_3 and 30.2% Na_2O, analytical grade), silica sol (28 wt % SiO_2 and 0.4 wt % Na_2O), and tetraethylammonium hydroxide (TEAOH) (30 wt % aqueous solution). The reaction mixture had the following molar composition: 8.4 TEAOH : 1.05 Na_2O : 1 Al_2O_3 : 30 SiO_2 : 540 H_2O. Hydrothermal crystallization was performed without stirring in autoclaves with Teflon liners at 170°C for three days. After washing with distilled water to a neutral reaction, the air-dry sample had the following chemical composition in terms of the molar composition of the zeolite Beta unit cell:

$$(NEt_4)_{4.41}Na_{0.74}[Al_{5.15}Si_{58.85}O_{128}] \cdot 9.08H_2O \cdot 0.63NEt_4OH.$$

The X-ray diffraction analysis (CuK_α radiation) of the resulting zeolite powder demonstrated that the diffraction pattern was fully consistent with the published diffraction patterns of zeolite Beta (Fig. 1). Lines due to foreign crystalline phases were not detected. According to scanning electron microscopy (SEM) data, an amorphous phase was absent from the sample, and the zeolite crystals were round polycrystalline agglomerates with an average size of about 1 μm.

IR Spectroscopic Studies

IR spectra were measured on a Shimadzu 8300 spectrometer over the range of 400–6000 cm^{-1} (resolution, 4 cm^{-1}; number of scans, 50). The samples for the IR spectroscopic studies were pressed as thin pellets (8–15 mg/cm^2) with no binder and heated at a chosen temperature in an IR cell in a vacuum or a flow of helium (2 l/h) for 2 h or in a flow of air (2 l/h) for 1 h followed by vacuum pumping for 1 h at the same temperature.

CO adsorption. Before the adsorption of CO, the sample temperature was decreased to 77 K by cooling with liquid nitrogen. To more accurately determine Lewis acid sites (LASs) of different strengths, the adsorption of carbon monoxide (CO) was performed with small portions (1.3, 5.3, 9.3, 13.3, and 400 Pa) to the complete saturation of surface sites, and the spectra of adsorbed CO were measured after each particular portion.

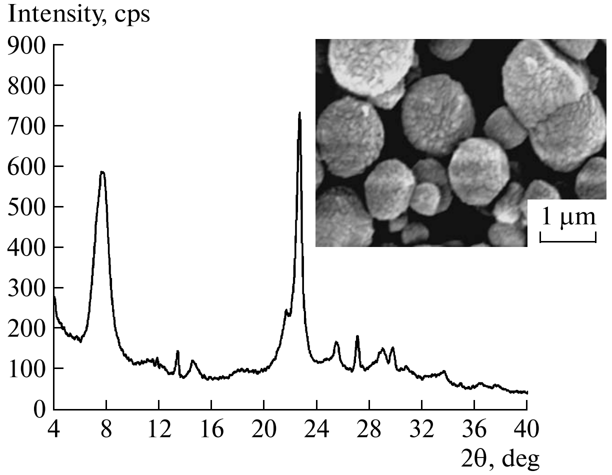

Fig. 1. X-ray diffraction pattern and SEM image of synthesized zeolite Beta.

The concentration (*C*, μmol/g) and strength of LASs (Q_{CO}, kJ/mol) were calculated from the intensity and position of bands due to CO adsorbed at –196°C [20] using Eqs. (1) and (2), respectively:

$$C\ (\mu mol/g) = (A_0\rho)^{-1}\int \log(T/T_0)d\nu, \qquad (1)$$

$$Q_{CO}\ (kJ/mol) = 10.5 + 0.5(\nu_{CO} - 2143), \qquad (2)$$

where A_0 is the integral absorption coefficient (cm/μmol); ρ is the pellet "thickness" (g/cm^2); T_0 and T are the IR radiation transmission coefficients (%) before and after CO adsorption, respectively; and ν_{CO} and 2143 are the frequencies of the stretching vibrations of the C–O bond in the adsorption complex (LAS) and the CO molecule, respectively.

The concentration of each particular type of LASs was determined with the use of integral absorption coefficients (A_0) published in [21].

The concentration of Brønsted acid sites (BASs) in zeolite channels was determined by two independent procedures: from the intensity of an band attributed to the OH^- group with a maximum at 3610 cm^{-1} using the coefficient $A_{0(OH)}$ = 7 cm/μmol [22] and from the intensity of an band attributed to this OH^- group in the H-complex with the CO molecule (maximum ν(OH–CO) = 3310 cm^{-1}) using the coefficient $A_{0(OH\cdots CO)}$ = 57 cm/μmol. The latter coefficient was specially measured in this work from the dependence of the specified band intensity on the amount of adsorbed CO, which was measured by a volumetric technique [22].

The concentration of BASs on the outer surface of a zeolite crystal (ν(OH) = 3730 cm^{-1}) was determined from the intensity of an band attributed to the OH group in the H-complex with the CO molecule (max-

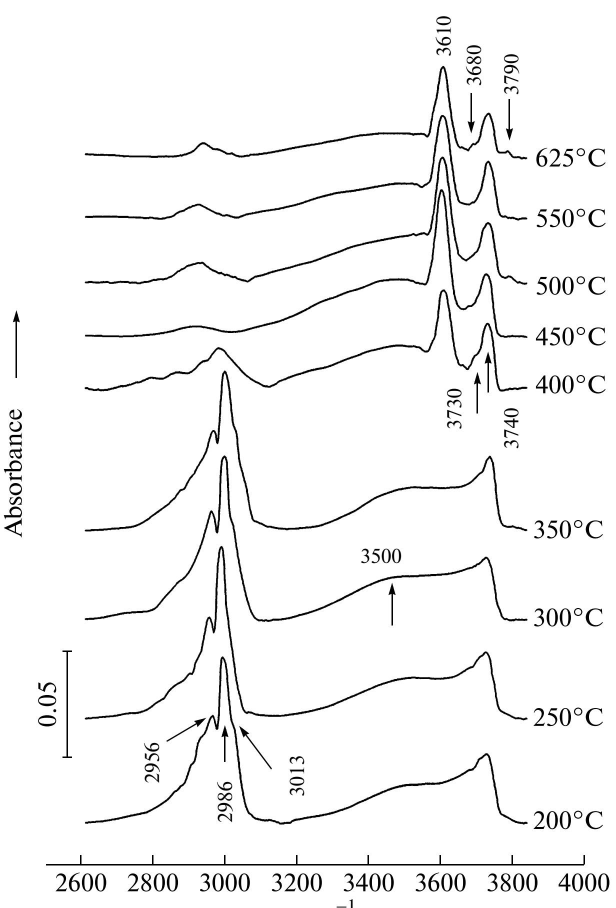

Fig. 2. IR spectra of zeolite Beta calcined in a vacuum at various temperatures (as specified in the figure).

imum ν(OH–CO) = 3430–3450 cm^{-1}) using the coefficient $A_{0(OH\cdots CO)}$ = 28 cm/μmol. In this case, $A_{0(OH...CO)}$ was obtained in a study of amorphous aluminosilicate from the dependence of the specified band intensity on the amount of adsorbed CO, which was measured by a volumetric technique [22].

The strength of proton sites was determined from the shift in the band attributed to structural OH groups in channels (ν(OH) = 3610 cm^{-1}) and on the outer surface of crystallites (ν(OH) = 3730 cm^{-1}) to the region of lower frequencies upon the formation of H-complexes with CO (ν(OH–CO) = 3310 and 3430–3450 cm^{-1}, respectively) [22].

NH_3 adsorption. The total concentration of acid sites in the samples of zeolite Beta calcined in a vacuum at various temperatures was determined from the adsorption of NH_3. Gaseous ammonia (10 ml) was adsorbed on a sample at room temperature, and an excess of ammonia was desorbed after 15 min at 100°C. The spectrum of adsorbed ammonia was measured at room temperature. The total concentration of BASs was calculated from the intensity of an band attributed to N–H vibrations in ammonium ions at 1450 cm^{-1} using $A_{0(NH)}$ = 10 cm/μmol [22].

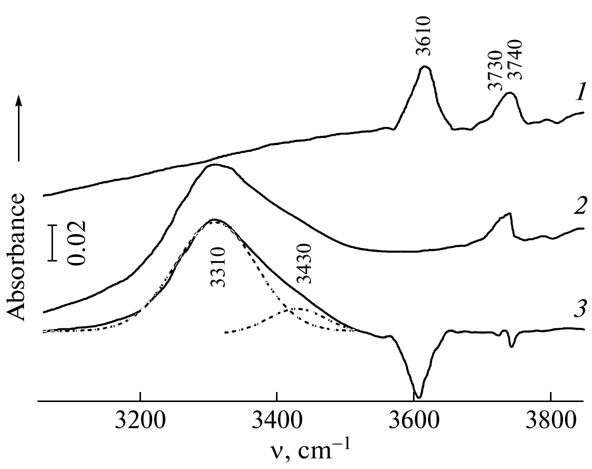

Fig. 3. IR spectra of the OH groups of zeolite Beta calcined in a vacuum at 450°C: (*1*) initial spectrum, (*2*) spectrum of a sample with CO adsorbed at –196°C, and (*3*) difference spectrum.

RESULTS AND DISCUSSION

Vacuum calcination. Figure 2 shows the IR spectra in the region of absorption due to the OH groups of zeolite Beta calcined in air at various temperatures. After the calcination of a sample in a vacuum at 200°C, the IR spectrum exhibited a few groups of bands: at 3740 cm^{-1} due to O–H vibrations in the SiOH group [23], a broad band at 3300–3500 cm^{-1} due to hydrogen-bonded acid OH groups [22, 24], and a band at 2850–3060 cm^{-1} due to C–H stretching vibrations in the alkyl fragments of the tetraethylammonium cation and its thermal degradation products.

At thermal treatment temperatures up to 350°C, considerable changes did not occur in the IR spectra of zeolite Beta (Fig. 2). A band at 3610 cm^{-1} due to the stretching vibrations of the bridging hydroxyl group

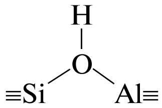
$\equiv Si-\overset{H}{\overset{|}{O}}-Al\equiv$ in zeolite channels and a band at 3730 cm^{-1} due to the stretching vibrations of the bridging hydroxyl group arranged at the outer surface of the zeolite Beta crystal [22] appeared in the spectrum only after calcination in a vacuum at 400°C. This was accompanied by a dramatic decrease in the intensities of bands due to C–H stretching vibrations in the alkyl fragments of the tetraethylammonium cation.

As an example, Fig. 3 shows a change in the spectra of OH groups in zeolite Beta calcined at 450°C (Fig. 3, curve *1*) upon the low-temperature adsorption of CO (Fig. 3, curve *2*). The difference spectrum obtained by subtraction of curve *1* from curve *2* (Fig. 3, curve *3*) indicates that the band at 3730 cm^{-1} shifted toward the low-frequency region to 3430 cm^{-1}, whereas the band at 3610 cm^{-1} shifted to 3300–3310 cm^{-1} because of the formation of the H-complexes of the CO molecule with bridging OH groups.

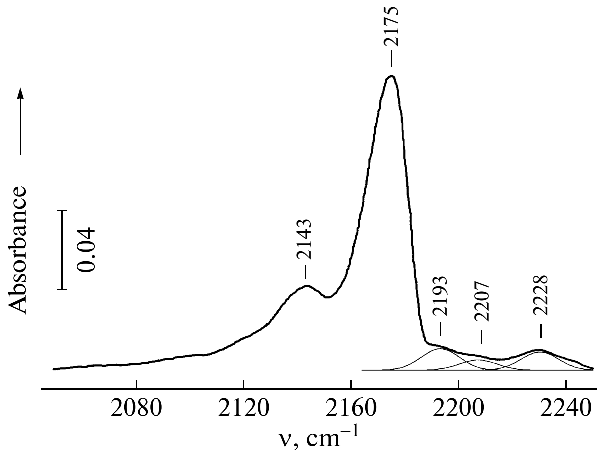

Fig. 4. IR spectrum of CO adsorbed at –196°C on the acid sites of zeolite Beta calcined in a vacuum at 450°C.

The shift of the bands due to OH, which characterizes the strength of BASs, was 290–300 cm^{-1} for the bridging OH groups of zeolite Beta (both within channels and arranged at the outer surface of crystallites). This value is approximately the same as that in the case of zeolite ZSM-5 (290–310 cm^{-1}), and it suggests that the BAS strength of zeolite Beta is close to the strength of the sites in zeolites from the group of pentasils [10–12].

The spectrum of adsorbed CO exhibited the following bands in the frequency range of 2000–2300 cm^{-1} (Fig. 4): a band at 2143 cm^{-1} due to physically adsorbed CO, a band at 2175 cm^{-1} with a shoulder at 2160 cm^{-1} due to the vibrations of CO molecules in complexes with hydroxyl groups, and three bands at 2193, 2207, and 2228–2230 cm^{-1} due to the vibrations of CO molecules that formed complexes with LASs (weak, medium, and strong, respectively) [22]. The position of the low-frequency band at 2193 cm^{-1} is close to the positions of the bands due to CO vibrations in complexes with LASs on the surface of γ-Al_2O_3. The appearance of this band in the spectrum of CO adsorbed on the surface of zeolite Beta can be due to the formation of Al_2O_3 phase nuclei in the course of thermal treatment.

Figure 5a shows the concentrations of BASs in zeolite Beta samples calcined in a vacuum at various temperatures. The concentration of hydrogen-bonded bridging OH groups, which are characterized by a band at 3300–3500 cm^{-1} and do not form H-complexes with CO, was not determined because the integral absorption coefficient is unknown for these bands.

In Fig. 5a, it can be seen that BASs were formed on the outer surface of zeolite Beta upon calcination at350°C and in the channels only at 400°C. The concentration of BASs reached a maximum value at 450°C; then, the amount of these sites gradually decreased to 250 μmol/g at 625°C.

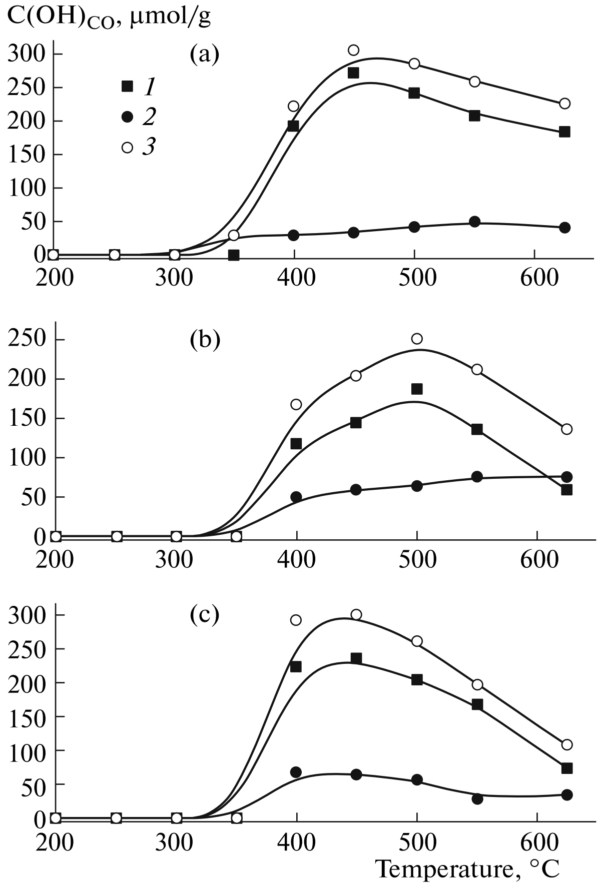

Fig. 5. The temperature dependence of the concentration of BASs in zeolite Beta samples calcined in (a) a vacuum, (b) air, and (c) helium: (*1*) OH groups in channels (ν(OH) = 3610 cm^{-1}), (*2*) OH groups on the outer surface (ν(OH) = 3730 cm^{-1}), and (*3*) the total concentration of BASs.

The concentration of LASs (Fig. 6a) dramatically increased upon calcination at 400°C and continued to increase as the temperature was further increased; this was mainly due to an increase in the amount of strong sites, whereas the concentrations of medium-strength and weak LASs remained approximately constant.

The highest concentration of acid sites obtained under vacuum thermal treatment conditions was 550 μmol/g. Based on the chemical composition of the initial form of zeolite Beta, this value should be of about 1115 μmol/g. It is most likely that sodium (160 μmol/g) from the initial form of zeolite replaced a proton in the BAS of the zeolite. Consequently, the expected maximum concentration of acid sites in the sample is 955 μmol/g. Thus, a considerable portion of acid sites (about 405 μmol/g or 42.4% in terms of possible chemical composition) was not determined with the use of CO as a probe molecule. It is believed that a portion of acid sites was blocked and was inaccessible to CO because of the incomplete removal of organic products from the zeolite upon heating in a vacuum.

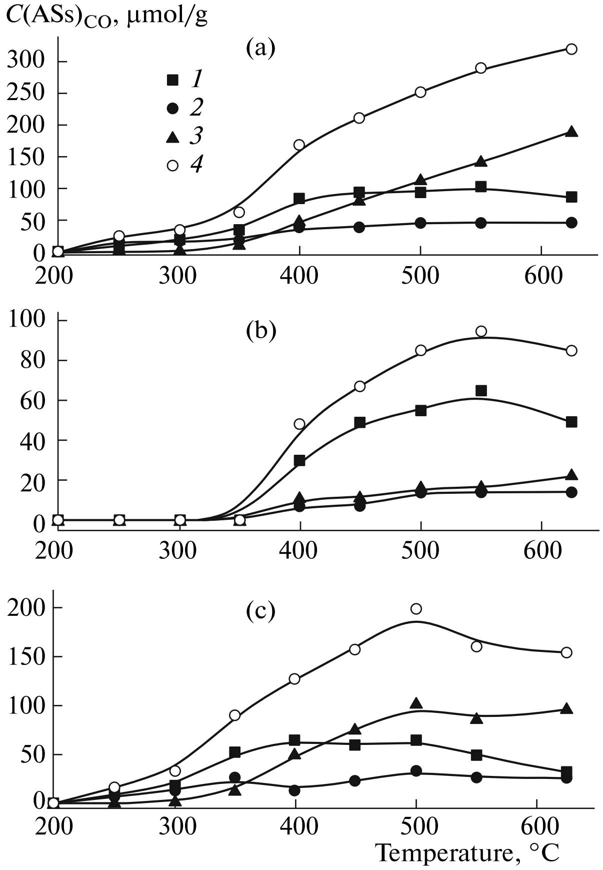

Fig. 6. The temperature dependence of the concentration of LASs in zeolite Beta samples calcined in (a) a vacuum, (b) air, and (c) helium: (*1*) weak (ν(CO) = 2190–2193 cm^{-1}), (*2*) medium (ν(CO) = 2205–2207 cm^{-1}), (*3*) strong (ν(CO) = 2228–2230 cm^{-1}), and (*4*) the total concentration of LASs.

To test this hypothesis, we performed the thermal treatment of zeolite Beta in a flow of air to facilitate the combustion of organic products.

Calcination in Flowing Air

Figures 5b and 6b illustrate data on the concentrations of acid sites formed upon the thermal treatment of zeolite Beta in a flow of air. A comparison between Figs. 5a and 5b and 6a and 6b exhibited a considerable difference between the results of the thermal treatments of zeolite Beta in a vacuum and in air. Thus, the concentration of LASs in the samples calcined in air was lower at any calcination temperature. The concentrations of BASs in the channels of the above samples were also lower; a maximum value of 240 μmol/g was reached at a temperature of 500°C. The thermal treatment conditions had almost no effect on the concentration of BASs on the outer surface of crystals. The total concentration of acid sites exhibited a maximum value of about 320 μmol/g, which is much lower than that in the case of vacuum thermal treatment.

Thus, in place of the expected increase in the concentration of acid sites due to the more complete combustion of the organic component of the initial zeolite form in air, we obtained an opposite situation. It is likely that the total acidity of the calcined zeolite decreased because of a local overheating and zeolite lattice degradation upon the combustion of the organic component. This is evident from the formation of alumina phase nuclei. The IR spectrum exhibited an band at ν(CO) = 2193 cm^{-1} and corresponding bands due to Al–OH groups at 3680 and 3790 cm^{-1}, which are analogous to those observed in samples calcined at 625°C in a vacuum (Fig. 1). In this case, the concentrations of BASs in the samples calcined at 500°C in air and at 625°C in a vacuum were similar.

The crucial difference between vacuum and air thermal treatments is in the removal of the organic component, namely, the tetraethylammonium cation, from zeolite channels. In the former case (in a vacuum), this is an endothermic process of the Hofmann degradation of the tetraethylammonium cation: ethylene and ethylamines in a protonated form are formed followed by the desorption of ethylamines into a gas phase under dynamic vacuum conditions and the formation of BASs. The possible formation of other triethylamine thermal conversion products (such as pyrrolidine and pyrrole [25]) in the channel space of zeolite Beta does not principally change the situation of the endothermic removal of organic components. In the latter case (in air), this is an exothermic process of the destructive oxidation of both the organic cation and its cleavage products; this may result in the local heating and partial degradation of the zeolite crystal. As a consequence, the probability of an escape of aluminum atoms from the zeolite framework increased (note that the tetraethylammonium cation was localized on the bridging oxygen atom at the framework aluminum), and the migration and association of extraframework aluminum cations to oxide phases were intensified to decrease the concentration of LASs. In addition, the concentration of BASs also decreased.

Calcination in Helium

To support the view that the heat of organic component decomposition on the surface and in the channels of zeolite Beta has an effect on the distribution of acid sites, we performed a series of experiments on the calcination of zeolite Beta samples at various temperatures in flowing helium. Data from this series are given in Figs. 5c and 6c. As can be seen in Figs. 5c and 6c, calcination in an inert atmosphere resulted in the formation of greater amounts of both BASs and strong LASs, as compared with calcination in an oxidizing atmosphere (Figs. 5b, 6b). The total amount of acid sites reached a maximum (460 μmol/g) at 500°C, and it was intermediate between those for vacuum thermal treatment and treatment in a flow of air.

Concentrations of acid sites (μmol/g) in zeolite Beta calcined in a vacuum, as determined using the adsorption of NH_3 and CO

Acid sites	Calcination temperature, °C								
	200	250	300	350	400	450	500	550	625
Localization of NH_4^+ ions	0	0	30	445	545	670	595	580	390
LASs on a CO basis	0	25	35	55	170	230	250	290	320
BASs on a CO basis	0	0	0	30	225	310	285	260	230
NH_4^+ + LASs	0	25	65	500	715	900	845	870	710
Intercrystallite OH groups*	0	0	30	415	320	360	310	320	160

* Determined from the difference between the concentrations of BASs measured using the adsorption of NH_3 and CO.

It is likely that the main difference between heating conditions in a vacuum and in helium consists in the diffusion inhibition of the removal of volatile decomposition products of the organic component (principally the same as those in the case of a vacuum) from the zeolite channel volume in the latter case. A decrease in the rate of removal resulted in an increase in the concentration of ethylene in the bulk of zeolite; in turn, ethylene was mainly adsorbed at strong Lewis sites and converted into undesorbed condensation products [26]. As a result of this, strong LASs, which were formed in the course of the thermal degradation of BASs, were blocked by ethylene condensation products and became inaccessible to CO molecules. Thus, unlike the situation of thermal treatment in a vacuum, where the decrease in BASs was compensated by an increase on the concentration of LASs and the total concentration of acid sites remained constant over the temperature range of 500–625°C, the total amount of acid sites decreased at high temperatures upon calcination in helium. This effect of temperature and the nature of a gas atmosphere during calcination on the distribution of acid site types was supported by the fact that the calcination of the initial form of zeolite Beta to 700°C in an inert atmosphere resulted in the incomplete removal of organic matter, small residues of which were detected by an exo effect of combustion after letting to air at 600°C [27].

Thus, it is most likely that an imbalance between the concentration of acid sites expected based on the chemical composition of the test sample and the total concentration of sites quantitatively determined by IR spectroscopic techniques with the use of CO as a probe molecule (channel and surface BASs and LASs) can be explained by the fact that a portion of BASs was localized at boundaries between the crystallites of zeolite Beta, and they formed hydrogen bonds. The space between two contacting crystallites was accessible to only the ammonia molecule with a kinetic diameter of 2.7 Å [28]. To test this hypothesis, we performed the adsorption of ammonia on zeolite Beta samples, which were thermally treated in a vacuum at various temperatures.

The table indicates that the total amount of acid sites found by summing BASs determined from the adsorption of ammonia and LASs was close to the possible value based on the chemical composition of the zeolite sample. These data also indicate that the main amount of NH_4^+ was formed after zeolite calcination at 350°C, that is, the same temperature at which almost all of the BASs were formed at the outer surface of zeolite crystals (see Fig. 5). Consequently, we can hypothesize that surface bridging hydroxyl groups participated in the formation of hydrogen bonds between crystallites. It is likely that, before calcination, both the channels and the external surface of individual zeolite crystallites were covered with tetraethylammonium ions. On calcination, the degradation of the tetraethylammonium ions began from the outer surface of crystallites. The resulting bridging OH groups of neighboring crystallites interacted with each other through the formation of H-bonds. The concentration of H-bonded OH groups and intercrystallite OH groups determined as ($[NH_4^+] - [BAS]_{CO}$) reached a maximum at 350°C; it somewhat decreased at 400°C and then remained almost constant to 550°C. Calcination at 625°C resulted in the condensation of the OH groups of neighboring crystallites and a decrease in the concentration of intercrystallite OH groups.

The experimental study of the acid–base properties of zeolite Beta performed by IR spectroscopy using CO and NH_3 molecules as probes demonstrated that the acid properties of the zeolite changed upon thermal treatments under the action of three factors. The first factor was the local overheating of individual zeolite crystallites in the course of the oxidation of organic templates or coke formation in channels or on the surface upon calcination in an inert atmosphere or in a vacuum. The second factor is well known [17–20, 22]: this is framework degradation under the action of temperature, which resulted in the escape of aluminum from the framework. The third factor is the migration of hydroxo aluminum fragments escaped from the framework to form oxygen aluminum clusters and alumina phase nuclei. Thus, changing the conditions of the calcination of the initial form of zeolite Beta (calcination temperature and/or atmosphere), we can affect these factors and regulate the qualitative and quantitative composition of acid sites. The quantitative comparison of the concentrations of sites determined by the adsorption of CO and NH_3 allowed us to conclude that the most reliable results were obtained with the use of CO or Py [22] as probe molecules. The use of the small strongly basic NH_3 molecule as a probe resulted in an overestimation of the total concentration of acid sites (see the table). In the calcination temperature region commonly used for catalyst preparation (400–550°C), this overestimation was about 40%.

REFERENCES

1. Perez-Pariente, J., Sastre, E., Fornes, V., Martens, J.A., Jacobs, P.A., and Corma, A., *Appl. Catal.*, 1991, vol. 69, p. 125.
2. Wadlinger, R.L., Kerr, G.T., and Rosinski, E.J., US Patent 3308069, 1967.
3. Treacy, M.M.J. and Newsam, J.M., *Nature*, 1988, vol. 332, p. 249.
4. Newsam, J.M., Treacy, M.M.J., Koetsier, W.T., and de Groyter, C.B., *Proc. R. Soc. London, Ser. A*, 1988, vol. 420, p. 375.
5. Perez-Pariente, J., Martens, J.A., and Jacobs, P.A., *Zeolites*, 1988, vol. 8, p. 46.
6. Leu, L.-J., Hou, L.-Y., Kang, B.-C., Li, C., Wu, S.-T., and Wu, J.-C., *Appl. Catal.*, 1991, vol. 69, p. 49.
7. Corma, A., Fornes, V., Melo, F., and Perez-Pariente, J., *Prepr.—Am. Chem. Soc., Div. Pet. Chem.*, 1987, p. 632.
8. Janin, A., Lavalley, J.C., Macedo, A., and Raatz, F., *ACS Symp. Ser.*, 1988, vol. 368, p. 117.
9. Corma, A., Fornes, V., Melo, F., and Perez-Pariente, J., *ACS Symp. Ser.,* 1988, vol. 375, p. 49.
10. Bourgeat-Lami, E., Massiani, P., Di Renzo, F., Espiau, P., and Fajula, F., *Appl. Catal.*, 1991, vol. 72, p. 139.
11. Maache, M., Janin, A., Lavalley, J.C., Joly, J.F., and Benazzi, E., *Zeolites*, 1993, vol. 13, p. 419.
12. Dimitrova, R., Gunduz, G., Dimitrov, L., Tsoncheva, T., Yialmaz, S., and Urquieta-Gonzalezeta, E.A., *J. Mol. Catal. A: Chem.*, 2004, vol. 214, p. 265.
13. Kubelkova, L., Beran, S., and Lercher, J.A., *Zeolites*, 1989, vol. 9, p. 539.
14. Zholobenko, V.L., Makarova, M.A., and Dwyer, J., *J. Phys. Chem.*, 1993, vol. 97, p. 5962.
15. Gora-Marek, K., Datka, J., Dzwigaj, S., and Che, M., *J. Phys. Chem. B*, 2006, vol. 110, p. 6763.
16. Zekai Zhang, Dong Liu, Xiangxue Zhu, Haiwei Yu, Shenglin Liu, and Longya Xu, *J. Nat. Gas Chem.*, 2008, vol. 17, p. 45.
17. Hedge, S.G., Kumar, R., Bhat, R.N., and Ratnasamy, P., *Zeolites*, 1989, vol. 9, p. 231.
18. Kotrel, S., Lunsford, J.H., and Knozinger, H., *J. Phys. Chem. B*, 2001, vol. 105, p. 3917.
19. Datka, J. and Gil, B., *Catal. Today*, 2001, vol. 70, p. 131.
20. Paukshtis, E.A. and Yurchenko, E.N., *Usp. Khim.*, 1982, vol. 52, no. 3, p. 426.
21. Soltanov, R.I., Paukshtis, E.A., and Yurchenko, E.N., *Kinet. Katal.*, 1982, vol. 23, no. 1, p. 164.
22. Paukshtis, E.A., *Infrakrasnaya spektroskopiya v geterogennom kislotno-osnovnom katalize* (Infrared Spectroscopy in Heterogeneous Acid–Base Catalysis), Novosibirsk: Nauka, 1992.
23. Vedrine, J.C., Auroux, A., and Condures, J., *ACS Symp. Ser.*, 1984, vol. 248, p. 253.
24. Zholobenko, V.L., Kustov, L.M., Borovkov, V.Yu., and Kazansky, V.B., *Zeolites*, 1988, vol. 8, p. 175.
25. Sauerland, C., Llewellyn, P., Grillet, Y., Patarin, J., and Rouquerol, F., *Proc. 12th Int. Zeolite Conf.*, Baltimore, 1999, vol. 3, p. 1707.
26. Stepanov, V.G., Paukshtis, E.A., Zaikovskii, V.I., Chesnokov, V.V., Ketchik, S.V., and Ione, K.G., *Proc. 8th Int. Zeolite Conf.*, Amsterdam, 1989, p. 447.
27. Perez-Pariente, J., Martens, J.A., and Jacobs, P.A., *Appl. Catal.*, 1987, vol. 31, p. 35.
28. Paukshtis, E.A., Romannikov, V.N., and Stepanov, V.G., *Primenenie tseolitov v katalize* (Catalytic Applications of Zeolites), Moscow, 1989, p. 18.